ACCEPTABLE WATER-OIL AND GAS-OIL RELATIVE PERMEABILITY MEASUREMENTS FOR USE IN RESERVOIR SIMULATION MODELS

Zubair Kalam, Tawfiq Obeida and Abdurrahman Al Masaabi
Abu Dhabi Company for Onshore Oil Operations, Abu Dhabi (UAE)

This paper was prepared for presentation at the International Symposium of the Society of Core Analysts held in Calgary, Canada, 10-12 September 2007

ABSTRACT

Representative relative permeability measurements and their use in validating reservoir simulation models is a key step in field development. Challenges faced are in choosing representative reservoir core samples and a consistency in the acquired experimental measurements at the relevant reservoir conditions. The choice of steady and unsteady state tests have been an on-going dilemma, coupled with uncertainty associated with high quality reservoir condition tests.

Our work with a prolific carbonate reservoir was focused to assess uncertainty and variations (if any) between steady (SS) and unsteady (USS) state full reservoir conditions water-oil relative permeability tests. Use of sophisticated in-situ saturation monitoring techniques and advanced core flood interpretations have shown that either technique can be used with confidence provided the level of heterogeneity is not too high to nullify the basic premise of the interpretations. Potential sources of errors are thoroughly examined using both the experimental techniques, with their consequent impact on dynamic model used in field development.

Gas-oil relative permeability is assessed by examining the errors and challenges in performing the tests at both ambient and at bubble pressure conditions. The impact of the gas-oil relative permeability tests and the ensuing data at different experimental conditions on gas displacement efficiency at miscible conditions are explored showing the significance of representative experimental design.

Properly designed reservoir condition tests during water-oil and gas-oil relative permeability determinations significantly reduce the uncertainty associated with many of the laboratory SCAL programs. A good focused program also minimizes the delays and costs associated with many of the extensive experimental measurements. The validity of the developed dynamic models in field development scenarios is used with confidence, minimizing an array of uncertainties.

INTRODUCTION

Representative and reliable relative permeability data obtained has significantly enhanced the validity of the developed simulation models. Consistency and repeatability in measured SCAL data is utmost important in validation of simulation models, and hence better management of reservoir development options. Previous studies have shown significant uncertainty in relative permeability data and end points, and consequently the

residual saturations. The paper outlines the field representative laboratory methods used, the recovery data obtained, and implications of the results on field developments plans.

This paper reports the results of water flood studies and immiscible gas floods performed on a prolific carbonate reservoir, as part of larger SCAL studies covering detailed Petrophysical measurements (capillary pressure, cementation and saturation exponents for representative cores at representative test conditions) and miscible gas process displacements. The objective of the water flood studies was to acquire and assess the impact of water/oil relative permeability data and validation of field development plans for possible development options. Various development options were studied to evaluate the optimum scenarios for the subject reservoir zone. Initial options focused on gas and / or water injection as the pressure maintenance fluid, and these were evaluated using a developed simulation model with analogue relative permeability curves. The SCAL data used in the development model was old, limited and did not cover the representative rock type identified in the static and geological models. Further, the existing data were acquired at ambient conditions and uncertainties existed in initial connate water saturation, wettability of the restored samples and the experimental deficiencies of the original measurements which were performed without in situ saturation monitoring, live oil aging and were not performed at full reservoir conditions.

The study objectives were to obtain representative reservoir dynamic data during water flood and gas flood for the reservoir simulation model in order to reduce reservoir model uncertainties. In order to minimise costs, and expedite on current uncertainties, the study involved a single rock type dominating the reservoir STOOIP, and where both water injection and gas injection play dominant roles in the management and proliferation of the reservoir.

RESERVOIR CORE DESCRIPTION

The reservoir rock type in question is easily identifiable on wireline logs with high porosity intervals dominated by matrix microporosity, with very few macrofauna or macroflora. It consists primarily of rare planktonic forams and fine skeletal debris surrounded by a uniform, chalky lime mud matrix. Texture ranges from lime mudstone-wackestone. Porosity varied from 18% to 30%, although the bulk of the plugs were around 22% to 28%, and permeability varied from 1 to 7 mD. The rock type is reasonably homogeneous, of poor-moderate quality reservoir, exhibiting variations due to degree of cementation near dense intervals and partial dolomitization. Thin Section photomicrographs confirm the presence of poorly connected microporosity, mainly dissolutional in nature but with isolated dissolutional and mouldic macropores, that limits the productivity of this rock type to only a few mD at best. High pressure mercury injection analysis of trims indicated unimodal pore throat distribution of 0.3 to 0.8 μm (predominantly 0.5 – 0.6 μm).

EXPERIMENTAL DETAILS

Core Preparation

The reservoir core samples used were plugged from preserved whole core samples acquired using low invasion non-damaging mud (water based). Representative reservoir core plugs were selected from X-Ray CT scanning of whole cores and plugs. Plugs that showed signs of local heterogeneity (vugs, high density inclusions, stylolites, fractures, etc) were omitted from SCAL testing. The reservoir core plugs were then prepared as follows:

1. The plugs were cleaned by warm solvent flushes of an azeotropic mix, toluene and methanol followed by saturation with synthetic formation brine and measurement of absolute brine permeability. The optimum cleaning technique was established earlier from a pre-study involving of five different techniques. SCAL plugs were never dried prior to relative permeability testing.
2. Plug pore volumes were measured using ISSM techniques by monitoring the miscible displacement of brine with doped brine.
3. Plugs were re-saturated to 100% brine and then de-saturated against a porous plate to representative values of irreducible water saturation (Swi). These were performed individually in core holders and the course of the de-saturations monitored by in-situ saturation monitoring (ISSM). Uniform or near uniform saturations were achieved.
4. Core composite of five plugs were prepared, ensuring that the plugs were of similar porosity and permeability within the chosen rock type.
5. The composites were transferred to a reservoir condition facility and the refined oil permeability at Swi measured. Following displacement of refined oil with dekalin, then stock tank oil (STO), the samples were raised to full reservoir conditions of approximately 300 barg and 121°C with a 40 barg net overburden pressure. At this stage the samples were flushed with live oil and aged for up to four weeks. Each week the live oil was displaced with fresh live oil and the permeability measured. At the end of the ageing period the live oil permeability value was then used as the reference permeability for the water-oil and gas-oil relative permeability measurements, respectively, on separate prepared composites.

The Displacement Tests

Pre-studies involved comparison of establishing Swi on individual plugs and composite of plugs. It was clear that uniform target saturations can be obtained very easily on individual plugs (de-saturated to approximately 0.20 PV) by Porous Plate, and that similar uniformity was not obtainable when the composite was de-saturated to target Swi using ISSM as depicted in Figure 1. Unsteady State (USS) water-oil relative permeability tests were performed on a core composite of five plugs (26.8 cm long with average porosity of 27.9%, Kw of 2.7 mD and Keo @ Swi of 2.9 mD) with the highest permeability at the top (outlet plug) and lowest permeability at the bottom (inlet plug) to minimise the effects of capillary pressure. The steady state (SS) measurement was performed on the same composite after secondary drainage, targeting Swi close to the

original value. The composite was first cleaned using the same sequence of hot miscible solvents, Swi set by drainage and then re-aged at full reservoir conditions. The water floods were performed with live crude at full reservoir conditions with in-situ saturation monitoring. Prior to the USS water flood, individual reservoir core samples were de-saturated to representative Swi values and reservoir wettability was restored. The relative permeability data were interpreted using core flood simulation software to correct for capillary pressure artefacts and/or assess the JBN analyses.

USS gas-oil relative permeability tests were performed on another composite of five brine saturated plugs prepared similar to the composite for the water/oil tests (as detailed above). The composite was prepared to Swi and aged with live crude to ensure restored wettability conditions. Composite length was 26.8 cm with an average porosity of 27.8%, Kw of 1.34 mD and Keo @ Swi of 1.36 mD. This was again assembled with the lowest permeability plug at the top (inlet end) and the highest permeability plug at the bottom (outlet end) to minimise capillary pressure end effects. Gas was injected from top to bottom to ensure gravity stable displacements, and same composite was used at both ambient and reservoir conditions (bubble point pressure) using ISSM. Single-speed centrifuge Kro and multi-speed centrifuge Pc data were also acquired on twin plugs of same RRT to improve the uncertainty in the measurements and correct for capillary pressure end effects. The USS test was repeated on same composite at both ambient and bubble point pressure conditions.

Unsteady State Water Flood

Water flood measurements were performed vertically bottom to top at three injection rates (to ensure gravity stable displacements), these being a reservoir advance rate of around 1ft/day, corresponding to a laboratory flow rate of around 3 mL/h and then two further rates at varying multiples of the low rate (corresponding to 9.6 ft/day and 26.6 ft/day). Figure 2 shows the ISSM scans at the start of the flood (at Swi), and at the end of the floods at three different rates. The high rate was chosen such that the maximum pressure drop across the sample was in the order of 250 psid. The water floods were performed directly after ageing, with no depressurization or movement of the core i.e. the whole process of ageing and water flood was performed sequentially on the same facility. Live brine was used which was doped with 5% NaI (sodium iodide) to ensure a density difference between the live oil/live brine, and thus allow the ISSM measurements. The core was scanned at the end of the ageing period and this scan defined the initial oil saturation at the start of the water flood. After the water flood the composite core samples were miscible solvent cleaned at test conditions and then flooded with doped live synthetic brine and live oil in order to measure the 100% pore volume calibration data for the ISSM technique. Saturation profiles were then derived for the water flood.

Steady State Water Flood

The SS water flood was performed on the same composite. As this was exactly the same composite used in the unsteady state water flood, direct comparisons of the data can be made. The USS composite was thoroughly cleaned and initialized to Swi, and then re-

aged at full reservoir conditions with live crude. After the unsteady state water flood, composite was oil flooded to measure secondary drainage K_{rw} and K_{ro}. Despite no porous plate in place, a reasonable residual water saturation profile was achieved, although its value (28.0% PV) was not as low as the original starting Swi (18.1% PV), which was derived from Porous Plate de-saturation of individual plugs. Sensitivity run of the SS test, involving numerical simulations to check the variation of Swi from 18 to 30% showed negligible impact on test results on current composite. This may be due to an assumption of constant wettability and negligible capillary end effects during the gravity stable fluid displacements at reservoir advance rates.

The SS test was performed at a total flow rate of 1.5ft/day, similar to the low rate flood in the USS displacement. The fractional flow rates of water (F_w) used were 1%, 5%, 10%, 20%, 50%, 70%, 90% and 100%. Each fractional flow was left until steady state was reached as judged by the ISSM measurements. The total duration of the steady state flood sequences (not including preparation of the core and unsteady state testing) was approximately 6 weeks.

Unsteady State Gas floods

The displacement rate of the injected gas was controlled by constant rate extraction of water from a large outlet accumulator (4 mL/h). The injected gas was supplied via a standard N_2 gas bottle connected to pressure reducing regulator and a backpressure regulator at the outlet end to control the desired constant rates. This was set to provide a constant inlet pressure and the gas was admitted to the core after passing through a saturator to ensure that gas was in equilibrium with oil at the injection pressure. Gas breakthrough occurred at 0.19PV due to possible viscous fingering, corresponding to a recovery of 23% HCPV. The overall impact of the fingering is likely to be minimal at the injected rates, and conversely significant if injected rates are too high. At the end of the low rate gas flood, the fractional flow of gas was 99.81%. The effective gas permeability was measured to be 0.03mD after 10 PV through put, corresponding to Krg of 0.022. The remaining oil saturation (ROS) was 0.60 HCPV (40 % HCPV recovery).

The gas flow rate was initially bumped to 24 mL/h (6 ft/day) for approximately 64 PV throughput. This rate was constrained due to high ΔP, since initially the oil saturation was still quite high (0.60 HCPV). The rate was then bumped to 359 mL/h (90 ft/day) for approximately 327 PV throughput. At the end of the medium and high rate gas floods, the effective gas permeability was measured to be 0.19 mD and 0.64 mD respectively. These effective permeabilities correspond to krg of 0.139 and 0.469. The final residual oil saturation was 0.30 HCPV (70% HCPV recovery).

RESULTS

Unsteady State Water Flood Results

An objective of the measurements was to provide end point relative permeability data and remaining oil saturation (ROS) data by using rigorous laboratory techniques. Remaining oil saturations (ROS) at the end of the reservoir advance rate flood (rate 1) of 6 PV throughput was 14.5% PV. The measured saturation change of 0.674 PV corresponded to

a low rate recovery of 82.4% HCPV. Brine break-through was observed at 0.6 PV (oil recovery at break through was equivalent to 73% HCPV).
At the end of the high rate floods the end point data shown are generally free of capillary end effects. Only very slight capillary pressure end effects remained as verified from the ISSM data (see Figure 2), therefore the ROS defined by the high throughput at the end of the high rate floods were accurate representations of expected residual saturations. There was 14.4% PV post breakthrough recovery to the end of the low rate, but from then on there was only a further 3.2% PV recovery to the end of rate 3 (i.e. ROS of 11.2%). The final saturation distributions were very uniform with negligible end effect.

Unsteady State Relative Permeability Analysis
The production and pressure drop data was first analyzed by the JBN technique. It was clear from the ISSM data that some of the measurements were subject to capillary pressure end effects, resulting in the JBN Kr curves being suppressed. Therefore the data was simulated using the *dyrect*SCAL method (Element and Goodyear, 2002). This software essentially allows an independent fit to pressure drop, oil production and in-situ saturation profiles to correct for the effects of capillary pressure, but without the need for an independent measure of imbibition capillary pressure. The resulting water and oil relative permeability curves are shown in Figure 3a. The Kro drops quite early after break through and the production increase with bumped rates are very small. It is important to note the narrow saturation range of post break through data obtained, and hence huge uncertainty in the constructed Kr curves. Such uncertainties are usually reduced by single-speed centrifuge data to extend the Kr curve over a wider saturation range, and rigorous use of ISSM data coupled with independent capillary pressure measurements (Masalmeh, 2003 and Spearing et al, 2004).

Steady State Water Flood Results
The saturation profiles from the SS test are shown in Figure 4. Also shown on this plot is the end point from the 1.5ft/day USS flood. Note that the final saturation at the end of the SS flood (83.2% PV) compares favorably to the USS saturation, providing reassurance on the ROS achieved. The SS relative permeability is robust in covering a much broader range of saturations and hence reduces the uncertainty typical of USS water floods with very narrow saturation changes from break through to end of the flood. Figure 3b shows the SS data together with the USS core flood simulation, USS measured end points and the oil displacing brine (secondary drainage) end points. As can be seen, a very good match between the SS and USS data was observed, enhancing the quality and consistency of overall data obtained. SS tests allowed acquisition of early flood data, prior to the breakthrough (compared with the USS data), and thus an improved definition of the relative permeability curves. The confidence in the SS data is further enhanced with the excellent match of measured data with simulated data, as shown in Figure 5 for ISSM and average brine saturations, respectively.

Ambient Condition Gas-Oil Relative Permeability Data

Gas-oil relative permeability curves have been estimated using JBN analysis. Following the low rate flood, additional equilibrium gas (equilibrated with dead crude) was prepared for high rate flooding. Use of equilibrium gas is important to minimise stripping effects of oil along the length of the composite. The injection rate was increased from an advance rate of 1ft/day to 6ft/day for 12 PV throughput followed by 90 ft/day for a further 18 PV throughput. The incremental oil production from the first bump was 0.05 PV. The second bump at 90ft/day produced a further 0.03 PV. The end-point scans are shown in Figure 6a. Excluding data from the first two plugs (0-0.11m), there was very little oil retention by end effect at the highest displacement rate, and hence the measured ROS of 0.29 PV (65% HCPV recovery) probably represents the maximum oil recovery. At the end of the ambient condition test, the composite core was degassed to restore refined oil at Swi. The composite was then moved to the reservoir condition facility.

Reservoir Condition Gas-Oil Relative Permeability Data

The composite core was initially aged at 3,500 psig at 121°C with STO (following displacement of the refined oil using dekalin). The composite core was reduced in pressure from 3,500 psig to the test pressure of 2,185 psig and the STO was displaced by equilibrium oil (equilibrated with gas at bubble point pressure). The test was conducted at the reservoir temperature of 121°C at a pressure of 2,185 psig. At this pressure, an equilibrium oil and gas mix could be prepared with the oil phase representative of the reservoir fluid i.e. at the reservoir fluid bubble point pressure. Using equilibrium gas to displace equilibrium oil should enable an immiscible flood to take place, free of compositional effects. At the initial oil saturation of 0.819 PV, the effective equilibrium oil permeability was measured to be 1.53 mD.

The low rate gas flood was conducted at a reservoir advance rate of 1 ft/day for a throughput of 6 PV. The pressure drop obtained is also a function of the average permeability and length of the composite. The throughput was constrained by the amount of equilibrium gas that could be prepared. Gas break through was observed after 0.31 PV of gas injection (38% HCPV recovery). At the low rate flood cessation, the measured in-situ oil saturation was about 0.37 PV (54% HCPV recovery). Figure 6 shows the complete measurements compared with numerically simulated data for in-situ saturation profiles, the pressure differentials applied, and the oil recovery. Possible experimental errors can arise from stripping effects of oil across the core length with variation in pressure drop. Figure 6d shows the impact of proper core flood simulation on recovery profiles, compared with simple JBN analysis that assumes negligible impact of capillary pressure end effects and a totally homogeneous core composite. JBN shows a constant or little further recovery beyond 5-6 PV of injected gas, while in reality production increases gradually all the way to approximately 200 PV. This result may have a major impact on the economics of the project as the former will imply no improvement in oil recovery beyond few PV's of gas injection while the latter shows an increase with gas injection.

Both the ambient and reservoir condition gas flood data are plotted in Figure 7. This comparison of data sets on the same composite shows that the reservoir condition test provides more optimistic Krg and Kro, the wetting oil phase showing more improvement than the non-wetting gas phase. Figure 7b compares the measurements with single-speed centrifuge Kro conducted at ambient conditions, and give an added measure of confidence in the derived Sorg. The single-speed centrifuge results show a steeper decline in Kro compared with USS displacements. This is somewhat unusual, and may be explicable in terms of choice of centrifuge speed, and more importantly the need for numerical simulation of centrifuge measurements as well as test being performed at reservoir temperatures and over burden pressure (experimental limitation). The difference in the data may also be the results of tests being done on different cores despite having a similar RRT.

The predicted viscosity ratio of the reservoir condition test was 0.05 (predicted equilibrium gas μg=0.018 cP and predicted equilibrium oil μo=0.350 cP) which was more favourable than the ambient condition test where the measured viscosity ratio was 0.009 (nitrogen gas μg=0.018cP and heavy-distillate μo=2.03 cP). Uncertainty in the predictions can be large at reservoir temperatures, and may have a more pronounced effect on the relative permeability curves. The capillary number, defined as ratio of viscous to capillary forces, i.e. $(\mu v)/\sigma$, for the reservoir condition test (measured IFT 4.2 mN/m) was 1.9×10^{-8} which was slightly higher than the ambient condition test of 0.3×10^{-8} (IFT ~25 mN/m). These flood parameters are similar, although for the reservoir condition test the flood characteristics are marginally better than for the ambient test. The ambient high rate end point data, as expected, appears to correctly measure reservoir Krg and Sorg.

IMPACT OF THE SCAL MEASUREMENTS

The water flood characteristics showed a mix between water wet and oil wet behaviour; the high breakthrough recovery and sharp increase in water cut post-breakthrough is indicative of water wet core but the post breakthrough recovery and Krw end points ranging from 0.3 to 0.6 is characteristic of intermediate to oil wet behaviour. Amott wettability tests on selected core plugs show it to be intermediate wet. The ROS from the water-oil SS test was only 2.3 % less than that measured on the USS state test at the same total flow rate of 1.5ft/day. An additional secondary water flood test on a much longer composite (53.5 cm) after initialization to target Swi (and prior to a tertiary gas flood) gave very similar oil recovery at water break through and final recovery at the end of the low rate flood (Cable et al, 2004). This provides confidence in the measured values and is reassuring that both techniques can provide essentially the same result, both in terms of relative permeability and final saturations. The USS and SS tests were performed on the same composite, comprising plugs of the reservoir rock type, and displayed intermediate wettability characteristics. The tests on the composite gave similar end-points and remaining oil saturation, despite the different experimental methodology.

As for the gas-oil displacements, the reservoir condition test provides more optimistic Krg and Kro, the wetting oil phase showing significantly more improvement than the non-wetting gas phase. Since these flooding parameters are very similar, they cannot

explain the observed significant improvement in Kro for the reservoir condition gas flood. The improvement in Kro might be a wettability phenomenon. From wettability measurements the cores are approximately neutral and mixed wettability. The injected, non-wetting gas phase, is analogous to a water flood on oil-wetting core. In this case one would expect to observe quite a low Kro curve for the ambient temperature test. Conversely, the non-wetting injected phase shows quite a high Krg curve. The observed improvement in Kro for the reservoir condition test is analogous to a more water-wet characteristic. There is no corresponding decline in injected phase relative permeability, since gas remains a non-wetting phase. The ambient and reservoir condition Krg are generally in agreement, particularly at the higher gas saturations where (Sg + Swi) > 0.6. Detailed impact of the reservoir condition test results on miscible gas injection performed with lean gas on a much longer composite (53.5 cm) are discussed elsewhere (Cable et al, 2004). The reservoir condition gas-oil Kr data were successfully used (despite the higher uncertainty in viscosity at higher temperature) to model secondary gas injection, tertiary gas injection and WAG displacements on the long composite, and validate the experimental results involving production data and effluent analysis using gas chromatography.

Figure 8 shows the recent water saturation difference map on top of the reservoir unit (del Sw = Sw using old SCAL – Sw using new SCAL). Using new SCAL data yields higher water at the flank area (negative del Sw), but lower water saturation on the crest area (positive del Sw). This means, that water in not moving as fast from flank to crest after using the new SCAL data, incorporating the combined USS/SS water-oil Kr and reservoir condition gas-oil Kr data. Using the new SCAL data yields lower water production (compared with old SCAL) from this reservoir unit as shown in Figure 9. During the early years of water production, the difference between the old and new SCAL is not so significant. At later years the difference between old and new SCAL gets bigger, and the model prediction is closer to observed water production. Thus the new data is less inconsistent with field observations, and enhances the validity of the developed model.

CONCLUSIONS

Representative reservoir conditions and rigorous laboratory experimental methods have been used to measure relative permeability and end point saturations. The data sets are consistent with themselves providing confidence in the measurements, and they are also consistent with independent wettability measurements. Combined SS and USS water-oil relative permeability tests with adequate core flood simulation and supplementary tests (such as single-speed centrifuge Kro and capillary pressure measurements) provide confidence in the obtained relative permeabilities and in the low remaining oil saturations measured. Although the two techniques gave similar results, uncertainty exists in deriving relative permeability curves from USS experiments of intermediate wettability samples unless a rigorous core flood simulation approach is used. Reservoir condition gas-oil relative permeability tests can enhance the obtained Krg and Kro although end point saturations can be similar to ambient condition measurements.

Use of valid relative permeability data significantly enhances the developed reservoir simulation model, and thus reduced uncertainty in the development options. Validation of observed field water production with dynamic model based on good SCAL data enhances the field development strategy.

ACKNOWLEDGEMENTS

This work was performed as part of SCAL Studies for the Abu Dhabi Company for Onshore Oil Operations (ADCO). ADCO and ADNOC management are gratefully acknowledged for permission to share the contents of this paper.

REFERENCES

Cable AS, Spearing M, Bahamaish J, Dabbour Y and Kalam MZ, "Gas Displacement Efficiency For a Low Permeability Carbonate Field", **SCA2004**-05, Abu Dhabi, 2004.

Element D and Goodyear S, "New Coreflood Simulator Based on Independent Treatment of In-situ Saturation and Pressure Data", **SCA2002**-07, Monterey, 2002.

Kalam MZ, El Mahdi A, Negahban S, Bahamaish JNB, Wilson OB and Spearing MC, "A Case Study to Demonstrate the Use of SCAL in Field Development Planning of a Middle East Carbonate Reservoir", **SCA2006-18**, Trondheim, 2006.

Masalmeh SK, "Studying the Effect of Wettability Heterogeneity on the Capillary Pressure Curves Using the Centrifuge Technique", *Journal of Petroleum Science and Engineering*, **33**, **29-38, 2002**.

Spearing MC, Cable AS, Element DJ, Goodfield M, Dabbour Y, Al Masaabi AR, Negahban S and Kalam MZ, "A Case Study of the Significance of Water Flood Relative Permeability Data for two Middle Eastern Reservoirs", **SCA2004-34**, Abu Dhabi, 2004.

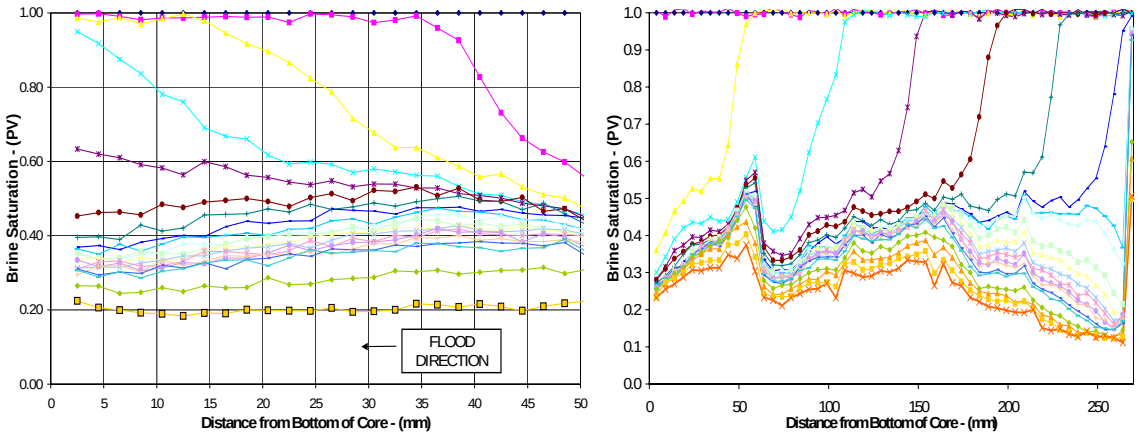

Figure 1. Comparison of Swi acquisition on a plug (left) and a composite (right)

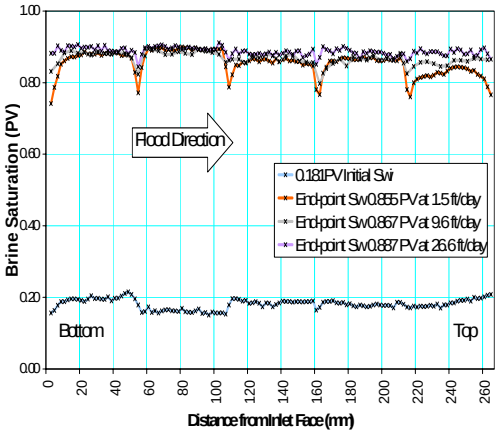

Figure 2. Swi and Sw profiles at the end of three different rates for USS water floods.

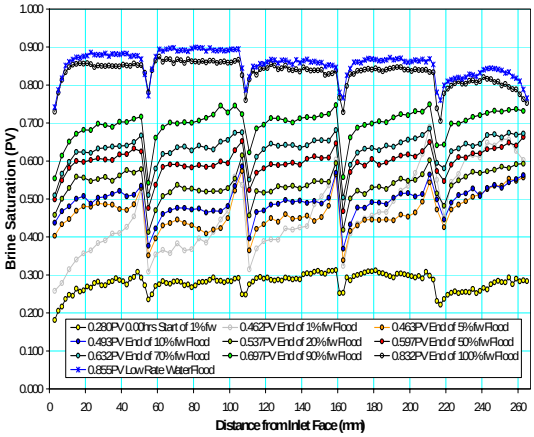

Figure 4. Steady state profiles for water flood and comparison with end of low rate USS flood at 1.5 ft/day.

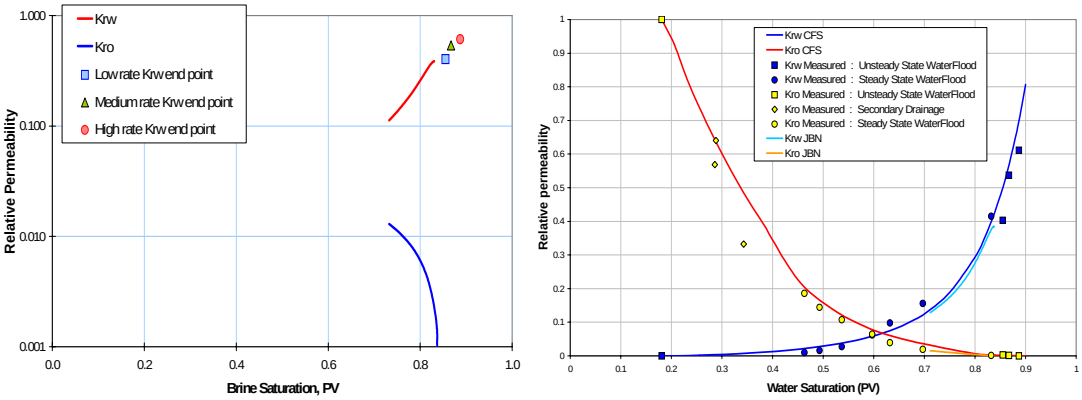

Figure 3. USS water flood on its own, and when combined with SS measurements

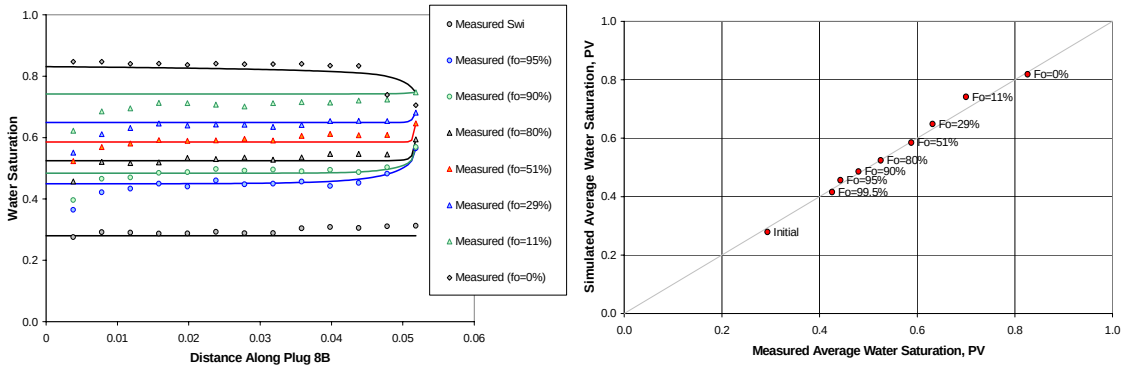

Figure 5. Simulated ISSM profiles and averaged brine saturation compared with the SS measurements

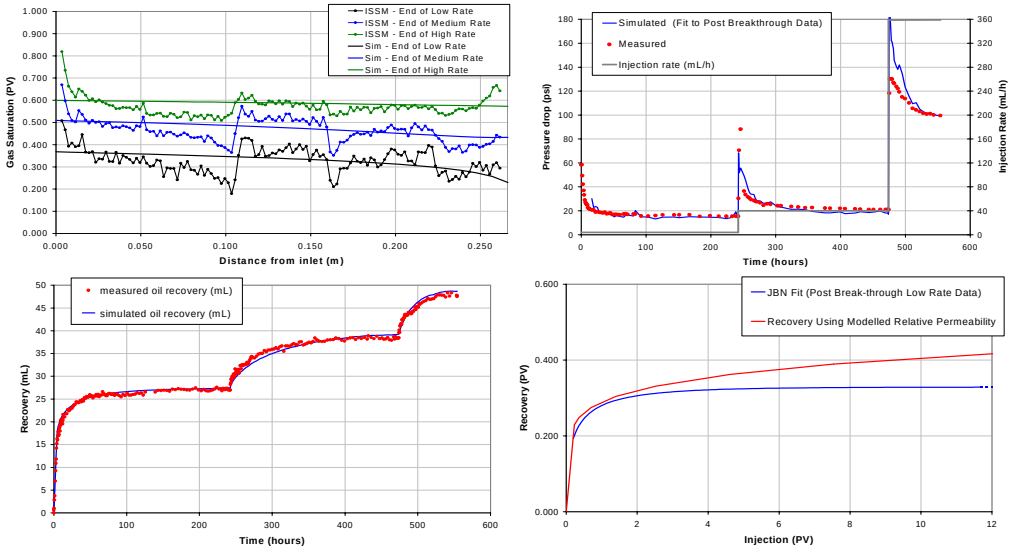

Figure 6. USS gas-oil relative permeability test on composite showing simulated and measured ISSM, dP and production at 3 rates, along with impact of simulation on JBN

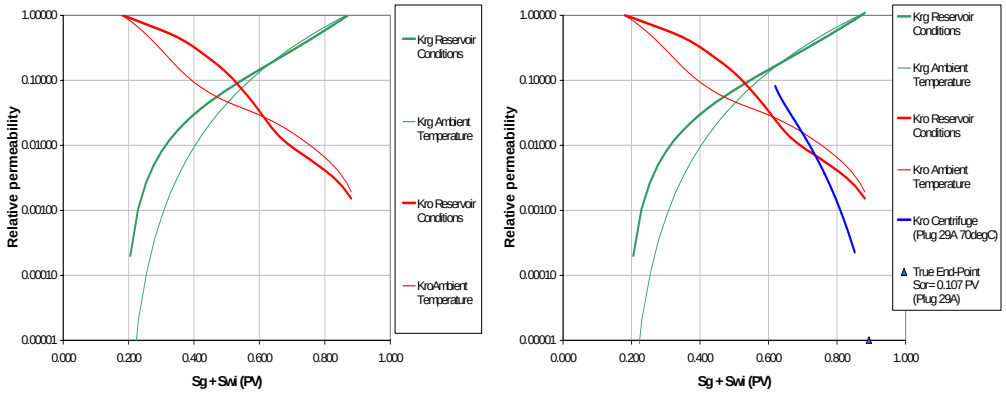

Figure 7. Gas/oil relative permeability curves at ambient and bubble point pressure conditions on same composite, and comparisons to centrifuge Kro.

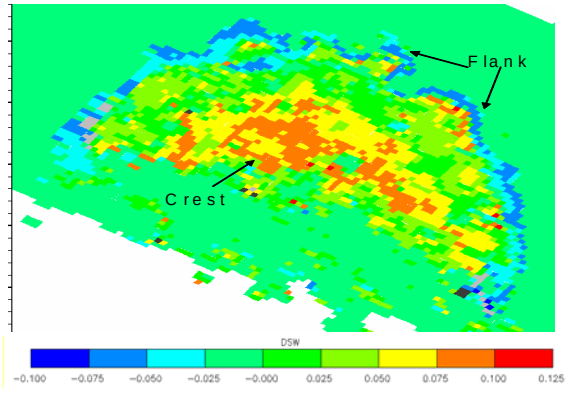

Figure 8. Water saturation difference map.

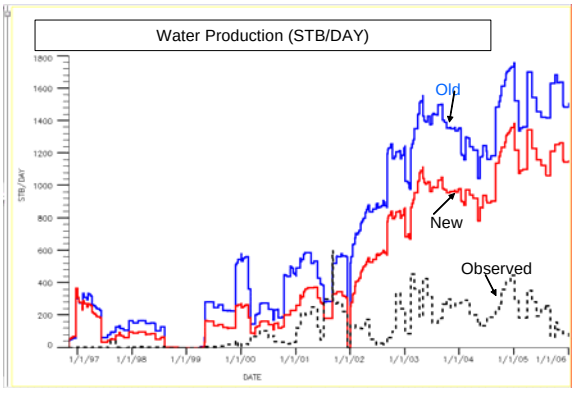

Figure 9. Water production from reservoir.